*Acta Cryst.* (1977). A33, 360–365

# Evidence for the Fankuchen Effect in Neutron Diffraction by Curved Crystals

BY G. ALBERTINI

*Facoltà di Medicina, Università di Ancona, Italy*

A. BOEUF AND S. LAGOMARSINO

*JRC Euratom, Ispra, Italy and Institut Laue–Langevin, 156X Centre de Tri, 38042 Grenoble, France*

S. MAZKEDIAN

*Facoltà di Ingegneria, Università di Ancona, Italy*

S. MELONE

*Facoltà di Medicina, Università di Ancona, Italy*

AND F. RUSTICHELLI

*JRC Euratom, Ispra, Italy; Institut Laue–Langevin, 156X Centre de Tri, 38042 Grenoble, France and Facoltà di Ingegneria, Università di Ancona, Italy*

(*Received* 29 *June* 1976; *accepted* 15 *November* 1976)

Experimental evidence of the Fankuchen effect for neutron diffraction by curved crystals is presented and discussed. The Fankuchen effect consists of a space condensation of neutrons (or X-rays) diffracted by an asymmetrically cut crystal. Theoretical considerations are presented on the Fankuchen effect in the case of ideal mosaic crystals, perfect crystals and ideal curved crystals. This analysis shows that mosaic crystals behave quite differently from perfect crystals. Whereas for perfect crystals the asymmetric cut is expected to induce a real gain in neutron current density, for mosaic crystals no gain is expected. Curved crystals are expected to behave in a similar way to perfect crystals. The experiments were carried out on chemically curved Si crystals. The neutron-diffraction characteristics of a symmetrically cut Si crystal and an asymmetrically cut Si crystal were compared. A gain in the neutron current density of a factor of 4 was observed in the case of the asymmetric crystal. This value is in good agreement with the estimated theoretical value of 4·2. This fact could lead to interesting applications in the selection of monochromatic beams to be used in neutron diffractometry of small biological crystals.

## Introduction

The first experiment on space condensation of X-rays due to asymmetric Bragg diffraction was performed by Fankuchen (1937) in connexion with measurements on tobacco mosaic virus. The principle of the condensing effect, which consists of the diffraction of an X-ray beam of area $S_1$ into a smaller area $S_2$, is shown in Fig. 1 and will be discussed below in more detail.

A more quantitative experiment of the same kind was performed by Evans, Hirsch & Kellar (1948), who reported peak reflectivities as a function of the asymmetry factor for calcite, quartz and fluorite crystals.

This paper will present experimental results concerning the Fankuchen effect in neutron diffraction by curved Si crystals. Some theoretical considerations will be given on the effects expected from ideal mosaic crystals, perfect crystals and ideal curved crystals, before the experimental data are presented and interpreted.

## Theoretical considerations

### (*a*) *Ideal mosaic crystals*

The propagation of Bragg-reflected neutrons by ideal mosaic crystals was treated extensively by Werner & Arrott (1965). They showed that for an infinitely large, incident neutron beam and an infinitely thick, non-absorbing mosaic crystal, the total neutron-diffracted power $P_H$ can reach a maximum value:

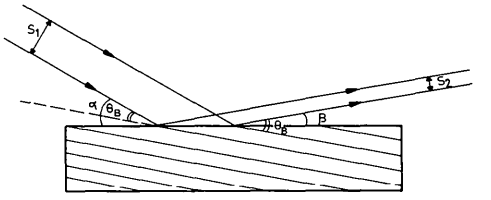


Fig. 1. Schematic representation of condensing effect in asymmetric Bragg reflexion.

$$P_H = P_0 \quad \text{for} \quad \gamma_0/\gamma_H \leq 1 \tag{1}$$

$$P_H = \frac{\gamma_H}{\gamma_0} P_0 \quad \text{for} \quad \gamma_0/\gamma_H > 1 \tag{2}$$

where $P_0$ is the incident neutron power at the given wavelength and $\gamma_0$ and $\gamma_H$ are defined by (see Fig. 1)

$$\gamma_0 = \sin \alpha \tag{3}$$

$$\gamma_H = \sin \beta. \tag{4}$$

On the other hand, from Fig. 1 it appears that the ratio $S_2/S_1$ of the two surfaces is equal to $\gamma_H/\gamma_0$. From the geometry, one could believe that the asymmetric cut induces a gain in the diffracted current density equal to the ratio $\gamma_0/\gamma_H$. However, from (2) it is apparent that the gain in the surface condensation is just compensated by the loss in the reflectivity, so that the current density in the diffracted neutron beam has the same value as in normal symmetric diffraction. On the other hand, the wavelength resolution $\Delta\lambda/\lambda$ of the diffracted beam is given by

$$\frac{\Delta\lambda}{\lambda} = (\cot \theta_B)\eta \tag{5}$$

in both the symmetric and asymmetric Bragg reflexion, $\theta_B$ being the Bragg angle and $\eta$ the mosaic spread.

(*b*) *Perfect crystals*

X-ray diffraction by perfect crystals is described by the dynamical theory reported by Zachariasen (1967) and others. Neutron diffraction by perfect crystals can, in practice, be described by the equations reported by Zachariasen (1967) for X-ray diffraction by non-absorbing crystals, as was shown by Goldberger & Seitz (1947). Obviously, a proper insertion of neutron physical quantities is necessary.

The dynamical diffraction profile of a perfect crystal can be expressed, as in Zachariasen (1967), in terms of the dimensionless units: $y$ and $A$. $y$ represents the angular orientation of the crystal, and $A$ the thickness of the crystal. For neutrons, the relation between $\Delta y$ and the angular deviation $\Delta\theta$ is

$$\Delta\theta = \frac{2F_H}{V_c \pi \tau^2} \tan \theta_B \left(\left|\frac{\gamma_H}{\gamma_0}\right|\right)^{1/2} \Delta y \tag{6}$$

where $F_H$ is the neutron structure factor, for the given reflexion, $V_c$ the volume of the elementary cell and $\tau$ the inverse of the interplanar distance. The relation between $A$ and the crystal thickness $t$ is

$$A = \frac{2F_H \sin \theta_B}{(|\gamma_0 \gamma_H|)^{1/2} \tau V_c} t. \tag{7}$$

The neutron diffraction pattern produced by a perfect crystal in Bragg geometry is given for the most general case (Zachariasen, 1967, p. 124) by

$$r \equiv \frac{P_H}{P_0} = \frac{1}{y^2 + (1-y^2)\coth^2 [A\sqrt{(1-y^2)}]}. \tag{8}$$

For $A \gg 1$, the diffraction pattern reduces to the well-known Darwin curve, which has an angular region of total reflexion of width equal to $2y$ and an integrated reflecting power $R_H^y$ in $y$ scale equal to $\pi$.

As the $A$ and $r$ definitions (7) and (8) are valid in the most general asymmetric Bragg case, it follows that for perfect crystals in the geometry shown in Fig. 1, $P_H/P_0 = 1$ for both $\gamma_0/\gamma_H > 1$ and $\gamma_0/\gamma_H \leq 1$. Therefore, if the crystal has an orientation corresponding to the centre of the Darwin curve, the condensing effect is real.

In practice, if one intends to use such a crystal as a monochromator, it is useful to compare the neutron intensity and the wavelength resolution with symmetric Bragg diffraction. In both symmetric and asymmetric Bragg diffraction, the reflectivity $P_H/P_0$ is equal to 1 inside the total reflexion region of the Darwin curve. Then the ratio $P_A/P_S$ of the total neutron power diffracted from the primary beam of surface $S_1$ for asymmetric ($A$) and symmetric ($S$) diffraction is given by the ratio of the corresponding wavelength resolution $\Delta\lambda_A/\Delta\lambda_S$. This ratio is obtained by replacing $\eta$ in (5) by the appropriate value for $\Delta\theta$ in (6). It is easy to see that

$$\frac{P_A}{P_S} = \frac{\Delta\lambda_A}{\Delta\lambda_S} = \sqrt{\left(\left|\frac{\gamma_H}{\gamma_0}\right|\right)}. \tag{9}$$

As the ratio between the surfaces $S_{2A}$ and $S_{2S}$ is given, for the same $S_1$, by

$$\frac{S_{2A}}{S_{2S}} = \frac{\gamma_H}{\gamma_0}, \tag{10}$$

if $J$ is the diffracted neutron current density, then

$$\frac{J_A}{J_S} = \sqrt{\left(\left|\frac{\gamma_0}{\gamma_H}\right|\right)}. \tag{11}$$

Therefore, perfect crystals behave quite differently from ideal mosaic crystals. An asymmetric cut in a perfect crystal introduces a gain given by (11) in the neutron current density. Furthermore, the wavelength resolution is increased by the factor given in (9).

In conclusion, the asymmetric perfect crystal acts as a condensing neutron lens. Therefore one expects that, as in a lens, the condensation of the flux in real space implies an increase of the angular divergence in such a way that the density in momentum space remains constant, in agreement with the Liouville theorem. In fact, there is an increase in the angular divergence, as discussed by Kohra & Kikuta (1968), who utilized the asymmetric cut in reversal conditions to obtain extremely parallel X-ray beams.

For a monochromatic beam, one obtains for the divergence of the secondary diffracted beam $\omega_H$ the following value:

$$\omega_H = \frac{\gamma_0}{\gamma_H} \omega_0. \tag{12}$$

$\omega_0$ is the divergence of the primary accepted beam (*i.e.* the angular width of the Darwin curve). For values of

$\gamma_0/\gamma_H$ of the order of 10, the value of $\omega_H$ remains lower than 1 minute and therefore is, in practice, negligible in comparison with the normal divergence of the incident white neutron beams.

(*c*) *Ideal curved crystals*

The neutron diffraction by ideal curved crystals was considered by Klar & Rustichelli (1973), who extended Taupin's (1964) X-ray dynamical theory. However, Albertini, Boeuf, Cesini, Mazkedian, Melone & Rustichelli (1976) have recently developed a simple model to describe the neutron diffraction by curved crystals, which is in agreement with the calculations of Klar & Rustichelli (1973). The advantage of their model is to allow a simple physical understanding of the phenomenon. In Klar & Rustichelli (1973) and in Albertini *et al.* (1976), a quantity $c$ related to the curvature of the crystal is defined as in Taupin (1964) to be

$$c=\frac{\mathrm{d}y}{\mathrm{d}A}. \tag{13}$$

From this definition, the following expression for $c$ can be derived for a spherically curved crystal

$$c=\frac{\pi\gamma_0 V_c^2}{2\lambda^3 F_H^2}\,\frac{2(b-1)[1+b\gamma_H^2(1+2k)]}{b\varrho} \tag{14}$$

where

$$b=\frac{\gamma_0}{\gamma_H},\quad k=\frac{\lambda^*}{\lambda^*+2\mu^*}$$

and $\varrho$ is the radius of curvature. ($\lambda^*$ and $\mu^*$ are the well-known Lamé coefficients.)

In (13), $y$ represents the deviation from the Bragg law at a certain depth $A$ below the surface of the crystal. If $y(0)$ is the deviation from the Bragg law at the surface of the crystal, then for a uniform curvature

$$y(A)=y(0)+cA\,. \tag{14}$$

In these units $c=1$ corresponds to the optimal curvature as discussed by Klar & Rustichelli (1973) and Albertini *et al.* (1976). From these two works it appears that, independently of asymmetry, for $c\leq 1$ the reflectivity $r=P_H/P_0$ is equal to one, in a range $\Delta y$ nearly equal to $cA$ (for $A\gg 1$):

$$\Delta y\simeq cA\,. \tag{15}$$

This means that the reflectivity is equal to one within an angular range which is nearly equal to the difference in the deviation from the Bragg law between the entrance surface and the back surface of the crystal. This angular range for a uniform spherical curvature is given in Taupin (1964) by

$$W=\frac{2(b-1)}{b\varrho}[1+b\gamma_H^2(1+2k)]\,\frac{t}{2\sin 2\theta_B}. \tag{16}$$

If one replaces in (5) $\eta$ with $W$, one obtains the wavelength resolution $\Delta\lambda/\lambda$.

The comparison will now be made between neutron diffraction by a symmetrically cut curved crystal with $c=1$ and an asymmetrically cut curved crystal (as in Fig. 1) also with $c=1$ (the radii of curvature of the two are not necessarily the same). Let us consider that the thicknesses of the two crystals are such that $W$, *i.e.* the wavelength resolution, is the same. As the reflectivity inside $W$ is 1 in both cases, the integrated reflectivity $R_H^\theta$ will be the same for both. As the ratio of the two surfaces is given by (10), the ratio of the diffracted current to neutron density will be

$$\frac{J_A}{J_S}=\frac{\gamma_0}{\gamma_H}. \tag{17}$$

Therefore, with regard to the Fankuchen effect, an ideally curved crystal behaves more like a perfect crystal than a mosaic crystal. However, comparing (17) with (11) it appears that the ratio $J_A/J_S$ is different for the perfect crystals and the curved crystals. This follows from the fact that for the perfect crystals there is an intrinsic difference in the resolution $\Delta\lambda/\lambda$ between the symmetric and the asymmetric reflexion (9), while for the curved crystals the comparison is made between a symmetric and an asymmetric reflexion with the same $\Delta\lambda/\lambda$.

## Experimental results and discussion

The measurements were carried out with perfect Si crystals which were curved by a microscopical technique described in Antonini, Corchia, Nicotera & Rustichelli (1972). A $Si_3N_4$ film was chemically produced at high temperature on one face of a perfect Si crystal 0·5 mm thick and 4 cm in diameter. By cooling the crystal, the difference in thermal expansion coefficient between Si and $Si_3N_4$ produces a uniform spherical curvature.

According to the theoretical analysis in the previous section, in order to compare the diffraction properties of symmetrically and asymmetrically cut curved crystals, the geometrical parameters of the two crystals should be chosen suitably. The $c$ values of both crystals

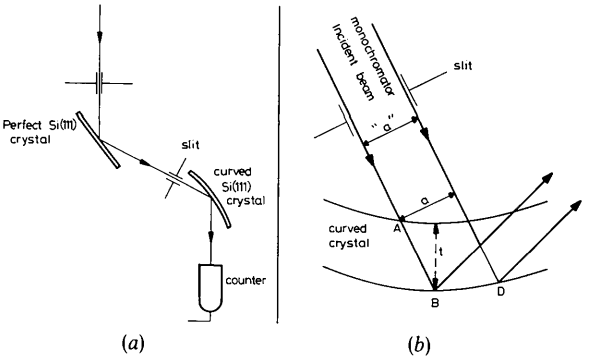


Fig. 2. (*a*) Experimental set-up. (*b*) Curved crystal with the impinging neutron beam.

must be equal to one. This implies that a proper choice of the radius of curvature [see (14)] is made for the chosen neutron wavelength at a given asymmetry factor $\gamma_0/\gamma_H$ and a given reflexion. Furthermore, the wavelength resolutions $\Delta\lambda/\lambda$ should be equal, which can be achieved by a proper choice of the crystal thicknesses.

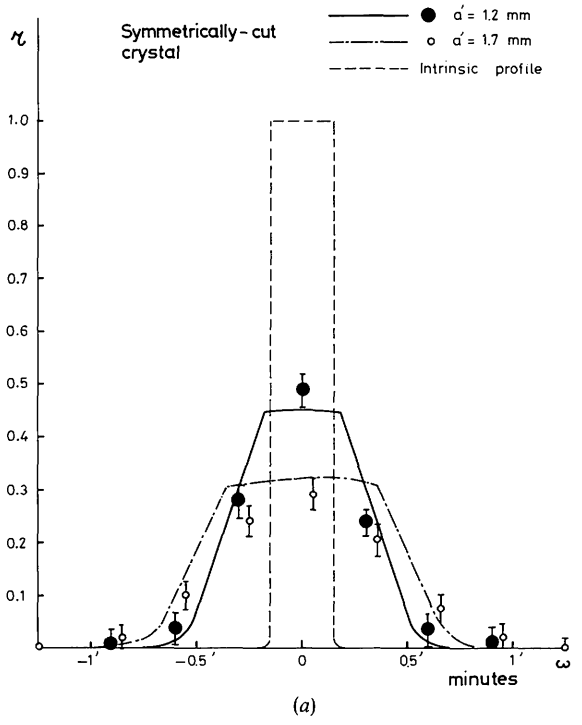


(a)

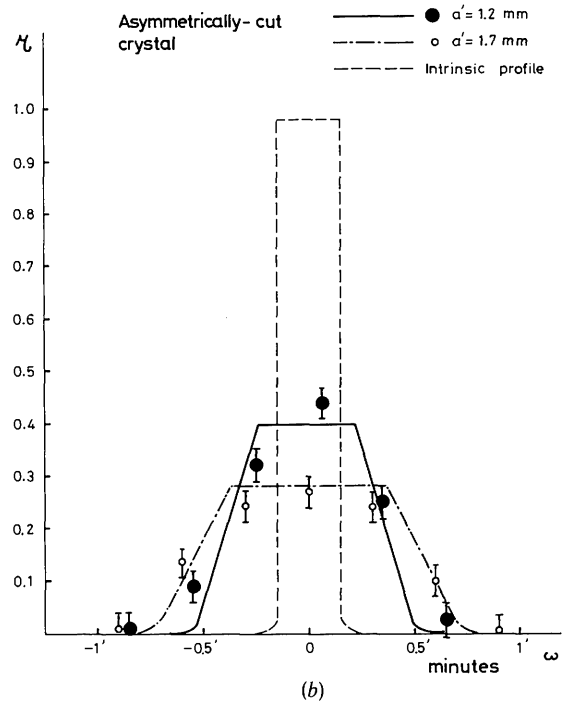


(b)

Fig. 3. Neutron diffraction pattern obtained at different beam width. Theoretical curve and experimental points for (*a*) symmetric and (*b*) asymmetric Bragg reflexion.

The experiments were performed at a neutron wavelength $\lambda = 1{\cdot}8$ Å corresponding to a Bragg angle $\theta_B = 16°$. The Si(111) reflexion was investigated. The asymmetric crystal was cut with the surface at 10° to the (111) plane which corresponds to a ratio $\gamma_0/\gamma_H$ equal to 4·2. In this case, the radius of curvature corresponding to $c = 1$ calculated according to (14) was $\varrho = 12{\cdot}5$ m. In practice, the experiments were performed with an asymmetric crystal having a radius of curvature $\varrho = 12$ m and a thickness of 0·5 mm, corresponding to $W = 0{\cdot}31'$ and $\Delta\lambda/\lambda = 3 \times 10^{-4}$. The symmetric crystal with the same $\Delta\lambda/\lambda$ value and the same $c$ value ($c = 1$) would have a radius of curvature $\varrho = 12$ m and a thicknes $t = 0{\cdot}33$ mm. However, for technical reasons, a crystal with a radius of curvature $\varrho = 20$ m and a thickness $t = 0{\cdot}5$ mm was utilized. Except for a small loss of intensity due to a negligible increase in absorption, the real symmetric crystal behaves like one with $\varrho = 12$ m and $t = 0{\cdot}30$ mm. In fact, both conditions $\varrho = 20$ m, $t = 0{\cdot}5$ mm and $\varrho = 12$ m, $t = 0{\cdot}30$ mm, lead to the same resolution $\Delta\lambda/\lambda$ and to the same peak reflectivity, nearly equal to 100%, because in both cases $c$ is smaller than or equal to one. Therefore, the real symmetric crystal behaves like the ideal crystal ($\varrho = 12$ m, $t = 0{\cdot}33$ mm) except for a slight difference in the $\Delta\lambda/\lambda$.

The first part of the experiment consisted in verifying the 100% peak reflectivity of the symmetric and asymmetric crystals and comparing the corresponding $\Delta\lambda/\lambda$. More precisely, the diffraction patterns of the two crystals were calculated with the model of Albertini *et al.* (1976) and are reported as dotted lines in Fig. 3. These two diffraction patterns will be called 'the intrinsic diffraction patterns'. The experiments were performed at the D13 diffractometer of the HFR Grenoble (Boeuf, Gobert & Rustichelli, 1975). Fig. 2(*a*) shows the experimental set-up. A perfect Si crystal utilized in symmetric Bragg reflexion gives a monochromatic beam. The diffraction patterns and the absolute reflectivities of both crystals were recorded. By using an infinitely narrow neutron monochromatic beam, the intrinsic diffraction patterns depicted in Fig. 3(*a*) and (*b*) should be obtained experimentally. However, the size of the neutron beam width, as it appears from Fig. 2(*b*), introduces a broadening of the diffraction pattern and a decrease in the peak reflectivity. The integrated reflecting power remains constant. In order to overcome this difficulty, several diffraction patterns for different neutron beam widths were recorded and an extrapolation procedure was used. The widths of the slit used to delimit the neutron beam were $a = 5$, 3·5, 1·5, 1, 0·6 mm. As the neutron beam had a certain divergence, and the slit was positioned at 20 cm from the crystal, the actual neutron beam width on the crystal itself ($a'$) was ~0·2 mm larger than the slit width.

The theoretical neutron diffraction patterns for a finite beam width can be obtained from the model of Albertini *et al.* (1976) by a simple adaptation and are reported in Fig. 3(*a*) and (*b*) for the $a' = 1{\cdot}2$ and $a' = 1{\cdot}7$ mm beam widths, together with the corresponding experimental points. The agreement is quite satisfactory.

The data corresponding to the other neutron beam widths are presented in a more synthetic form in Fig. 4. In particular, the figure reports, for each neutron beam width, the experimentally observed full width at half maximum, the maximum reflectivity $r = P_H/P_0$ and the integrated reflecting power $R_H^\theta$, as well as the theoretical predictions of the model for these three quantities, in both the symmetric and asymmetric Bragg reflexions. A satisfactory agreement appears between experimental data and theoretical predictions. It can thus be foreseen that with an infinitely narrow neutron beam, one would obtain a similar agreement of the experimental results with the intrinsic diffraction profiles for the two crystals.

After that verification, the crystals were positioned in a neutron white beam ($8 \times 12$ mm$^2$) at the Bragg angle corresponding to $\lambda = 1{\cdot}8$ Å. A picture of the two diffracted beams is reported in Fig. 5. A horizontal scan of the counter in a direction perpendicular to the two diffracted beams was performed using a $1 \times 1$ mm$^2$ slit. The result of this scan is reported in Fig. 6. From Figs. 5 and 6, the condensation effect due to the Fankuchen cut is evident. The value of the experimental ratio $J_A/J_S$ deduced from Fig. 6 is $4{\cdot}0 \pm 0{\cdot}3$, which is in good agreement with the 4·2 value expected from (17). These results may lead to useful applications of curved crystal monochromators in neutron diffractometry of very small (to 1 mm$^3$) biological substances. However, other facts, such as, for instance, the focusing effect due to the curvature of the crystals, must be considered in a practical application.

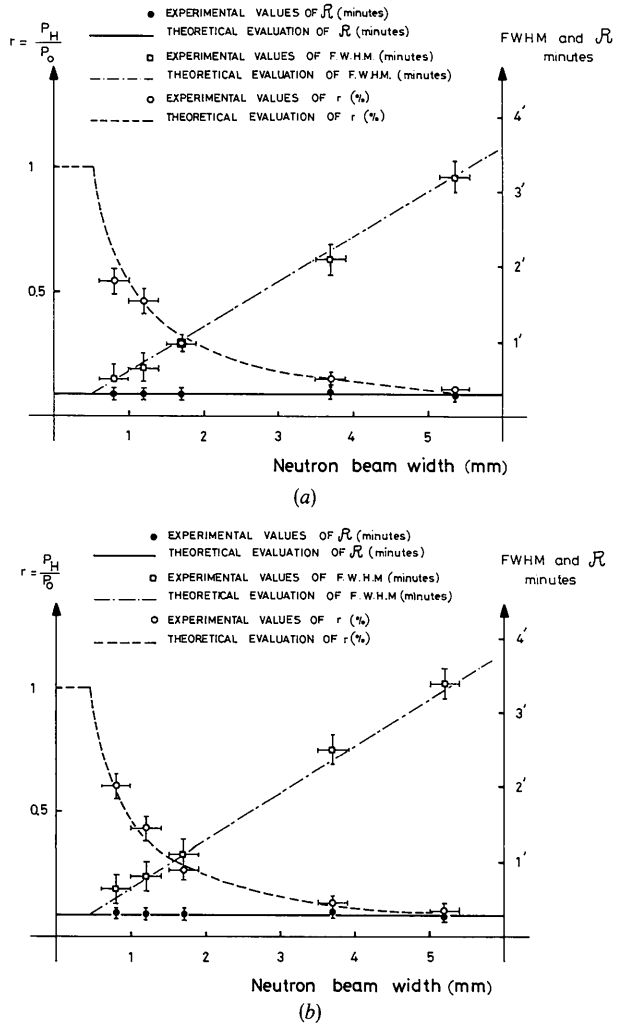


Fig. 4. Neutron maximum reflectivity ($r$), neutron integrated reflectivity ($R$) and full width at half maximum (FWHM) of the diffraction patterns as a function of the neutron beam width (*a*) for a symmetric Bragg reflexion and (*b*) for an asymmetric Bragg reflexion.

## Conclusions

The Fankuchen effect was observed in the neutron diffraction by curved Si crystals. This effect consists of a space condensation of the diffracted neutrons due to an asymmetric cut of the crystal which corresponds to an increase in the neutron current density equal to the asymmetry factor. The gain observed of $4{\cdot}0 \pm 0{\cdot}3$ agrees quite well with the theoretical value of 4·2 for the given geometry. A theoretical analysis of this effect is also

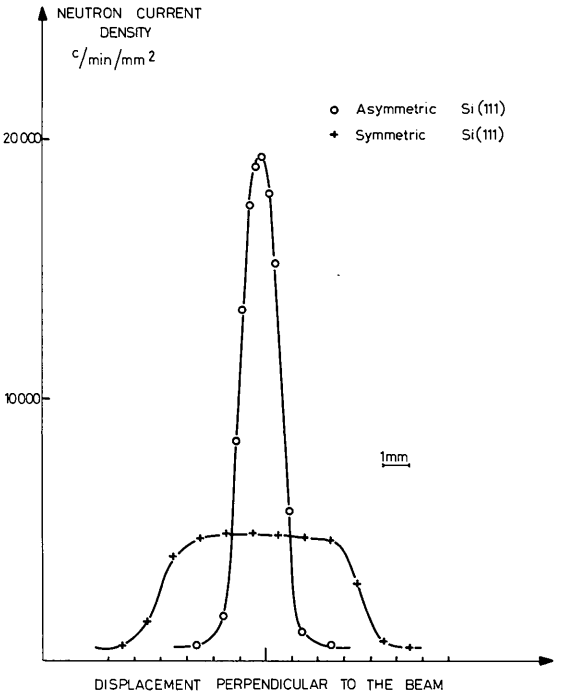


Fig. 6. Horizontal scan of the neutron current density of the symmetrically and asymmetrically diffracted neutron beams.

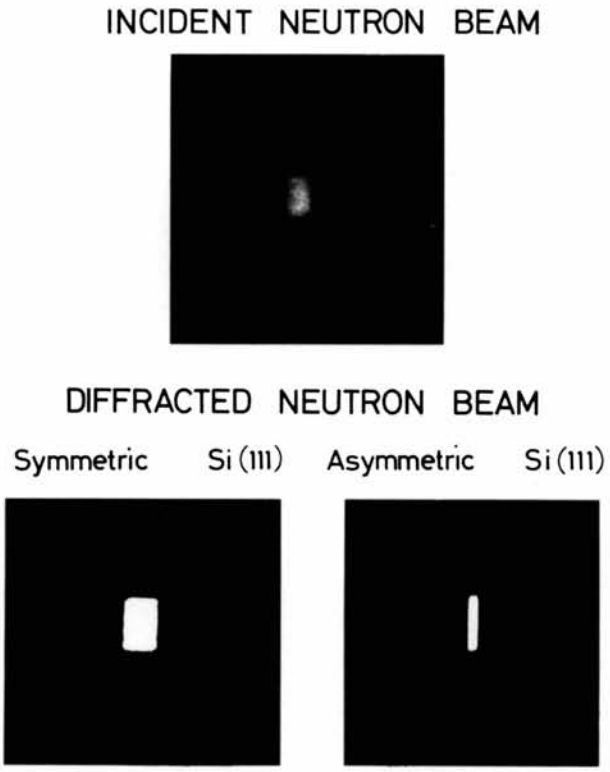


Fig. 5. Picture of the symmetrically and asymmetrically diffracted beams.

[*To face p.* 364

reported for perfect and mosaic crystals. In particular it is shown, following Werner & Arrott (1965), that for mosaic crystals, contrary to that for perfect crystals, the condensation effect is compensated by a loss of reflectivity of the same factor.

In conclusion, this experiment, on one hand, constitutes a verification of some predictions of the dynamical theory of neutron diffraction, and, on the other hand, opens interesting perspectives to increase the neutron intensities in the diffractometry of small biological samples.

### References


ALBERTINI, G., BOEUF, A., CESINI, G., MAZKEDIAN, S., MELONE, S., RUSTICHELLI, F. (1976). *Acta Cryst.* A**32**, 863–868.

ANTONINI, M., CORCHIA, M., NICOTERA, E. & RUSTICHELLI, F. (1972). *Nucl. Instrum. Meth.* **104**, 147–152.

BOEUF, A., GOBERT, G. & RUSTICHELLI, F. (1975). *Nucl. Instrum. Meth.* **124**, 533–540.

EVANS, R. C., HIRSCH, P. B. & KELLAR, J. N. (1948). *Acta Cryst.* **1**, 124–129.

FANKUCHEN, I. (1937). *Nature, Lond.* **139**, 193–194.

GOLDBERGER, M. L. & SEITZ, F. (1947). *Phys. Rev.* **71**, 294–310.

KLAR, B. & RUSTICHELLI, F. (1973). *Nuovo Cim.* **13B**, 249–271.

KOHRA, K. & KIKUTA, S. (1968). *Acta Cryst.* A**24**, 200–205.

TAUPIN, D. (1964). *Bull. Soc. Fr. Minér. Crist.* **87**, 469–511.

WERNER, S. A. & ARROTT, A. (1965). *Phys. Rev.* **140**, 2A, 675–686.

ZACHARIASEN, W. H. (1967). *Theory of X-ray Diffraction in Crystals*. New York: Dover.


*Acta Cryst.* (1977). A**33**, 365–367

# A Structure Factor Equation for Structures Consisting of Point Scatterers with Known Minimum Distance


BY R. ROTHBAUER

*Institut für Kristallographie und Mineralogie der Universität Frankfurt*, 6 *Frankfurt/Main* 1, *Senckenberg-Anlage* 30, *Germany (BRD)*


(*Received* 28 *May* 1976; *accepted* 25 *October* 1976)


For unitary, normalized and neutron structure factors the equation:

$$0=\sum_{\mathbf{m}} A(\mathbf{h},\mathbf{m})F(\mathbf{m})F(\mathbf{h}-\mathbf{m})$$

with

$$A(\mathbf{h},\mathbf{m})=F(\mathbf{m},\beta_{11})F(\mathbf{h}-\mathbf{m},\beta_{12})F(\mathbf{h},\beta_{21}\beta_{22})-F(\mathbf{m},\beta_{21})F(\mathbf{h}-\mathbf{m},\beta_{22})F(\mathbf{h},\beta_{11}\beta_{12})$$

is valid, where the $F(\mathbf{m},\beta_{\mu\nu})$ are the form factors of arbitrary artificial density functions $\beta_{\mu\nu}$, which are not more extensive than a sphere of diameter equal to the minimum atomic distance of the structure.


Since the early days of X-ray crystallography many attempts have been made to find procedures for the formulation of structure-factor relations, because these can be used as determinantal relations for the unknown phases and hence for structure analysis by direct methods.

A formalism to derive structure-factor equations, which are exactly valid for arbitrary crystals with known chemical content, was first developed by Woolfson (1958) by generalizing the equation of Sayre (1952). The multiple sums of these equations, which make practical application difficult, disappear if one replaces in Woolfson's theory the generating mappings, $\varrho^j(\mathbf{x})$, $j=1,2,\ldots$, of the scattering density, $\varrho(\mathbf{x})$, by linear combinations of $D_{\nu 1}\varrho D_{\nu 2}\varrho$, $\nu=1,2,\ldots$, where $D_{\nu 1}$ and $D_{\nu 2}$ are differential operators (Rothbauer, 1975, 1976).

In the following such a procedure is applied to a practical important degenerate case.

## The equation

The electron density distribution, $\varrho_\mu(\mathbf{x})$, $\mu=1,2,\ldots$, of many kinds of atoms differs by a factor, which may be assumed to be constant for the purposes of structure analysis. There are therefore many crystal structures, whose scattering density function:

$$\varrho(\mathbf{x})=\sum_{\mu=1}^{p}\sum_{\nu=1}^{q(\mu)}\varrho_\mu(\mathbf{x}-\mathbf{x}_{\mu\nu}) \tag{1a}$$

can be written approximately in the form:

$$\varrho(\mathbf{x})=\sum_{\mu=1}^{p}\sum_{\nu=1}^{q(\mu)}f_\mu\beta(\mathbf{x}-\mathbf{x}_{\mu\nu}), \tag{1b}$$

where $\beta(\mathbf{x})$ is a function characteristic of the shape of the atoms of the structure, $p$ equals the number of different kinds of atoms, $f_\mu$ and $q(\mu)$ describe the scattering density and the number of atoms of kind $\mu$, respectively, and $\mathbf{x}_{\mu\nu}$ denotes the position of the $\nu$th atom of the $\mu$th kind.

If one introduces a distribution:

$$\tau(\mathbf{x})=\sum_{\mu=1}^{p}\sum_{\nu=1}^{q(\mu)}f_\mu\delta(\mathbf{x}-\mathbf{x}_{\mu\nu}) \tag{2}$$

with a scattering density concentrated at the points $\mathbf{x}_{\mu\nu}$, one can express $\varrho$ as the convolution of $\tau$ and $\beta$: